

Lola V. Sichugova<sup>1</sup>, Dilbarkhon Sh. Fazilova<sup>2</sup>

**STRUCTURAL INTERPRETATION OF LINEAMENTS  
USING SATELLITE IMAGE PROCESSING:  
A CASE STUDY IN THE VICINITY OF THE CHARVAK RESERVOIR**

**ABSTRACT**

This work presents the results of lineaments interpretation using the automated method of the satellite images in the territory of the Charvak water reservoir in Uzbekistan. Tectonic and local (water impoundment in Charvak reservoir) features of the region deformation were determined on base LINE algorithm in software PCI Geomatica. The thematic map with the geospatial arrangement of lineaments was constructed on base of satellite images LANDSAT-8 processing. We concluded that water level fluctuations have a greater influence on the appearance of the lineaments structure than periods of water filling and downstream in the reservoir. Lineament density maps showed dominantly increased density towards the north-southern direction is due to tectonic features of the region and the west-eastern direction is due to water level fluctuations in the reservoir. The lineaments density maps for summer-autumn periods showed the faults arising from water level fluctuations only. Winter-spring period affected with high influence of the seasonal (snow pack, rainfall) processes as well.

**KEYWORDS:** lineaments, LINE algorithm, LANDSAT-8, line density, Charvak reservoir

**INTRODUCTION**

Currently, a significant development was given by satellite observation methods of geodynamic processes. The operational analysis of geodynamics by recording the variability of lineaments on selected satellite images is one of the advanced methods for monitoring tectonically active territories [Bondur *et al.*, 2009]. Lineament analysis was used to study active fault patterns in unreachable mountain areas [Chaabouni *et al.*, 2012] and for analysis of underground water dynamics [Takorabt *et al.*, 2018]. Remote sensing techniques are highly informative, in particular, for assesment of the geodynamic environment state near artificial water reservoirs [Gubin, 2010]. Territories with a high density of lineaments is unsuitable for the construction of dams and reservoirs as the possibility of water leakages into the subsurface, slope and dam failures and rate of sedimentation would be higher [Prabhakaran, Jawahar, 2018]. This work describes the method and the results of the analysis of lineaments structures by interpretation satellite data of the Landsat-8. The vicinity of Charvak water reservoir was chosen for analysis of deformations due to tectonic movements and water level fluctuations in the reservoir processes.

**Study Area**

The Charvak water reservoir is located in the Middle Tien-Shan zone at the boundary the Tien-Shan orogenic territory and the Turan plate. The mountain ranges (Karzhantau, Chatkal and Kurami), covered by young structures in some areas, surround this field and decrease in southwest direction. Recent up thrusts and deflections characterize plain part of the territory [Yarmuhamedov *et al.*, 1979].

In 1970, construction of the Charvak dam with the height of 167 m has ended and started flowage of Brichmulla depression and filling of the reservoir. Along the 1000 km river's length

---

<sup>1</sup> Ulugh Beg Astronomical Institute (UBAI) of the Uzbekistan Academy of Sciences, Astronomicheskaya str., 33, Uzbekistan, Tashkent; *e-mail*: [slola988@gmail.com](mailto:slola988@gmail.com)

<sup>2</sup> Ulugh Beg Astronomical Institute (UBAI) of the Uzbekistan Academy of Sciences, Astronomicheskaya str., 33, Uzbekistan, Tashkent; *e-mail*: [dil\\_faz@yahoo.com](mailto:dil_faz@yahoo.com)

between the Toktogul and the Chardarya reservoirs, Charvak and two other main reservoirs (Karakul, Andijan) are included to the Naryn–Syrdarya-cascade. The reservoir surface area is about 40 km<sup>2</sup> and its capacity is 2 km<sup>3</sup>. Water reservoir intends mainly for hydro-power purposes [Rakhmatullaev *et al.*, 2013]. High mountainous regions are located in the south-east and north near Charvak water reservoir and the maximum heights reaches up to 3000 m.

## MATERIALS AND METHODS OF RESEARCHES

The free-availability of global coverage Landsat-8 data provides the opportunity for medium resolution global land surface monitoring [Roy *et al.*, 2014]. The Landsat-8 satellite is in circular sun-synchronous orbits and, with the 15° Operational Land Imager (OLI) sensor field of view with 16-day repeat cycles. The Landsat-8 images with 30 m resolution of the study region from the United States Geological Survey (USGS) Earth Explorer website were obtained for special (top water level, downstream, fully drawn down) time periods in the Charvak reservoir (December, March, June and September). The Landsat-8 has 11 reflective wavelengths (from 435 nm to 12510 nm) bands, 7 of them (coastal, blue, green, red, NIR, SWIR 1/2) were used in this study.

Automated lineament analysis methodology was used in this research. Data analysis carried out using ENVI, PCI Geomatica and ArcGIS software. The first step of the methodology is the selection of initial input data for lineament extraction. Image processing for the extraction of lineaments involving multi-bands image, contrast stretching, and image enhancement. Principal Component Analysis (PCA) was carried out on the satellite data using ENVI software. PCA was created with seven multi-bands images. It is used to de-correlate the different bands and to reduce the dimension of the resulting feature space enhancing the multi-band image for structural interpretation purposes. The goal was to use inter-band correlation, to compress textural information from the seven co-occurrence images and to represent nearly the whole of the available information. Fig. 1 shows the result of the PCA of the study area.

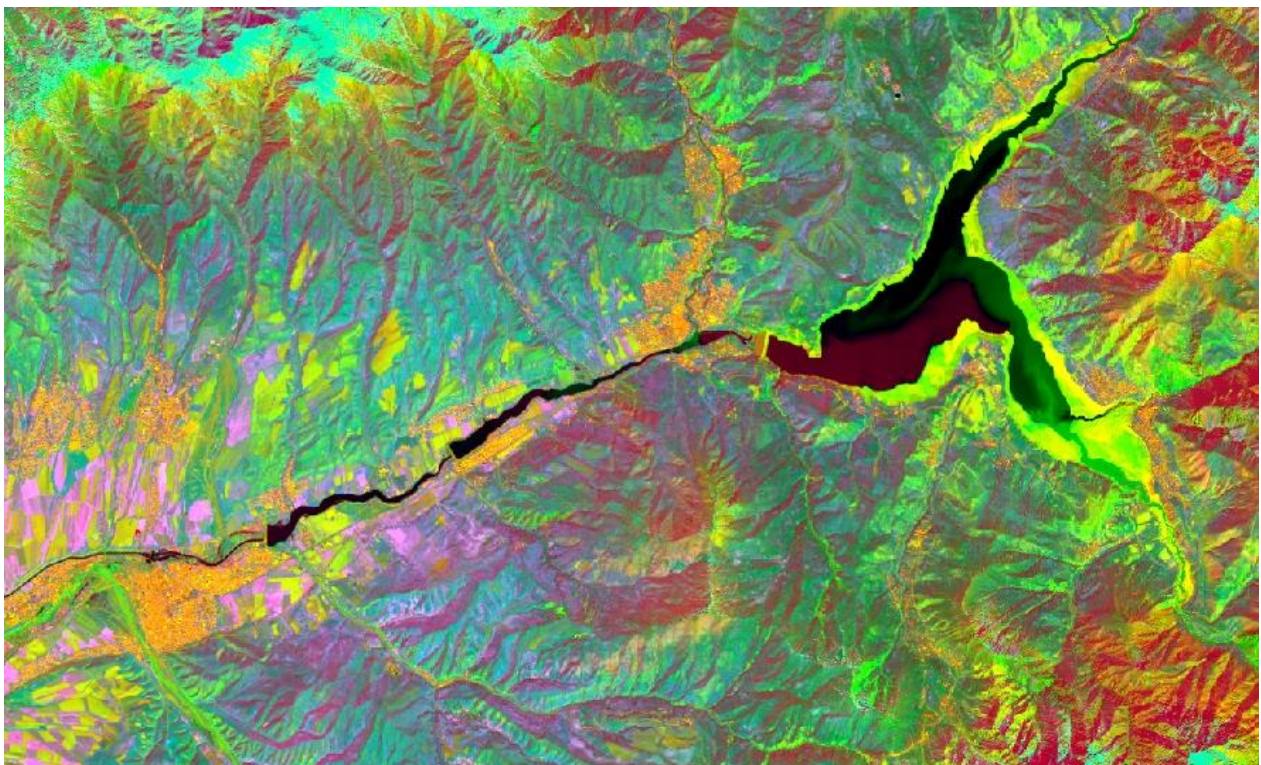


*Fig. 1. PCA of the study area in March 2016*

The analysis of the automatic extraction of lineaments was done using the LINE module of PCI Geomatica [Geomatica, 2013]. The principle of operation of the module is to extract linear objects from the raster images and the output lines are saving in vector format. The final poly-lines are saved in a vector segment. The algorithm parameters used for processing are as follows:

1. **RADI** — Radius of the filter in pixels;
2. **GTHR** — Threshold for edge gradient;
3. **LTHR** — Threshold for curve length;
4. **FTHR** — Threshold for line fitting error;
5. **ATHR** — Threshold for angular difference;
6. **DTHR** — Threshold for linking distance.

The LINE algorithm consists of three main processing steps: edge detection, thresholding and curve extraction. In the first step, the Canny Edge detection algorithm is applied to produce an edge strength image. There are three sub steps: filtering the input image using the Gaussian functions with a radius according to the parameter Filter Radius (RADI), gradient calculation and, finally, pixels whose gradient are not the local maximum are suppressed by setting the edge strength to 0. In the second stage, the edge strength image is a threshold to obtain a binary image. The threshold value is defined by the Edge Gradient Threshold (GTHR) parameter. And, finally, the last stage, curve extraction, consists of producing pixel-wide skeleton curves, extracting of a sequence of pixels for each curve and converting them to vector format by fitting line segments to it. The maximum fitting error (distance between the two) is specified by the Line Fitting Threshold (FTHR) parameter. And finally, the algorithm links pairs of polylines that satisfy the conditions:

- Two end-segments of the two polylines face each other and have similar orientation (the angle between the two segments is less than the value specified by ATHR);
- The two end-segments are close to each other (the distance between the end points is less than the value of DTHR).

The parameters of the algorithm are presented in table 1. The length and rose diagrams of the lineaments of automatically extracted were also calculated. The lineament density parameter was built in ArcGIS using the density tool. This instrument calculates the density of linear facilities in each cell of the exit grid.

*Table 1. Parameters of the LINE Algorithm*

<b>№</b>	<b>Name</b>	<b>Description</b>	<b>Unit</b>	<b>Data range</b>	<b>Value</b>
1	RADI	Filter Radius	Pixels	0–8192	10
2	GTHR	Edge Gradient Threshold	—	0–255	50
3	FTHR	Line Fitting Threshold	Pixels	0–8192	30
4	LTHR	Line Fitting Threshold	Pixels	0–8192	3
5	ATHR	Angular Difference Threshold	Degrees	0–90	15
6	DTHR	Linking Distance Threshold	Pixels	0–8192	20

## **RESULTS OF RESEARCHES AND THEIR DISCUSSION**

Linear features on a satellite image regularly reflect the geological lineaments (faults or fractures) and hydrological structures (river or shoreline) [Lillesand *et al.*, 2004]. The lineaments were extracted from the PCA image to show distinct structural features (including faults, shears and fractures). The fig. 2 and table 2 present statistics (maximum and minimum length, density and orientation) of lineaments for different time periods. Results show that the minimum of

lineaments numbers reached in December month (2250) during reservoir end of water downstream time. In contrast, March, June and September are periods with high numbers of lineaments. It is possible that water level fluctuations have a greater influence on the appearance of the lineaments structure than periods of water filling and downstream in the reservoir.

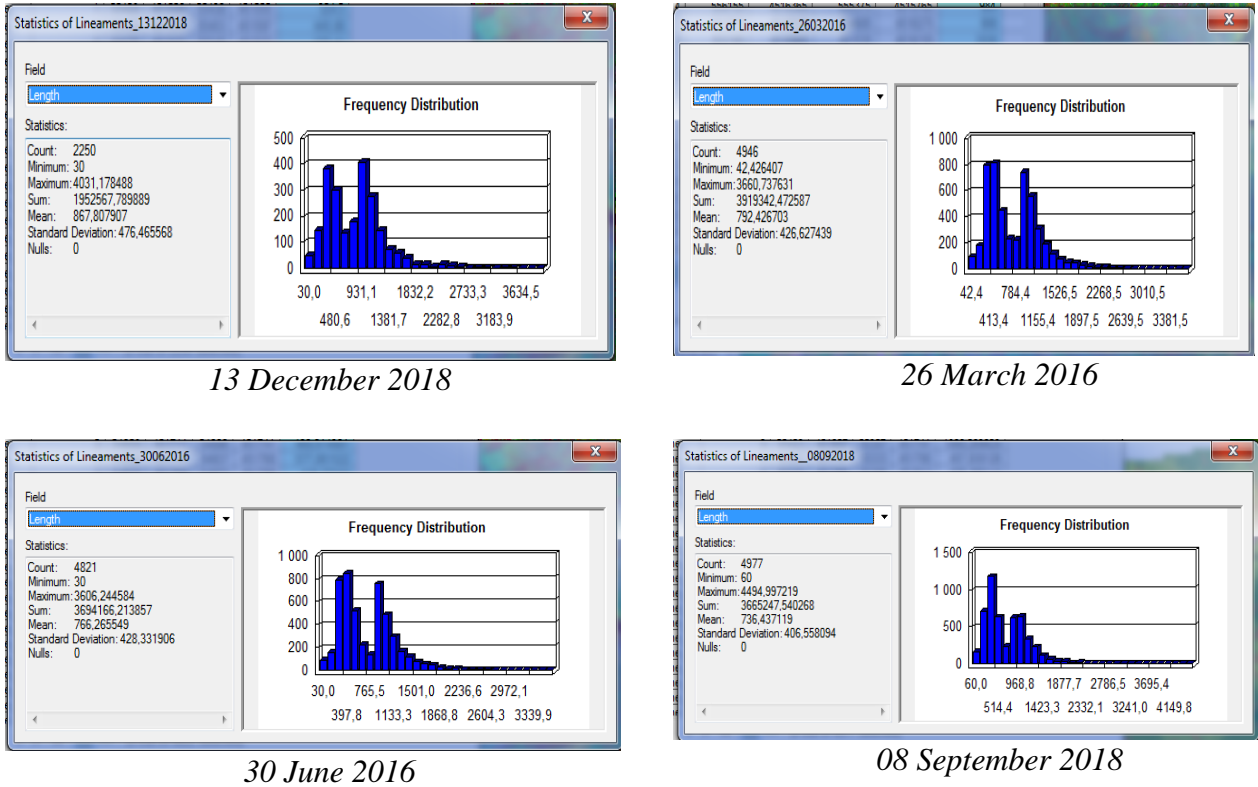


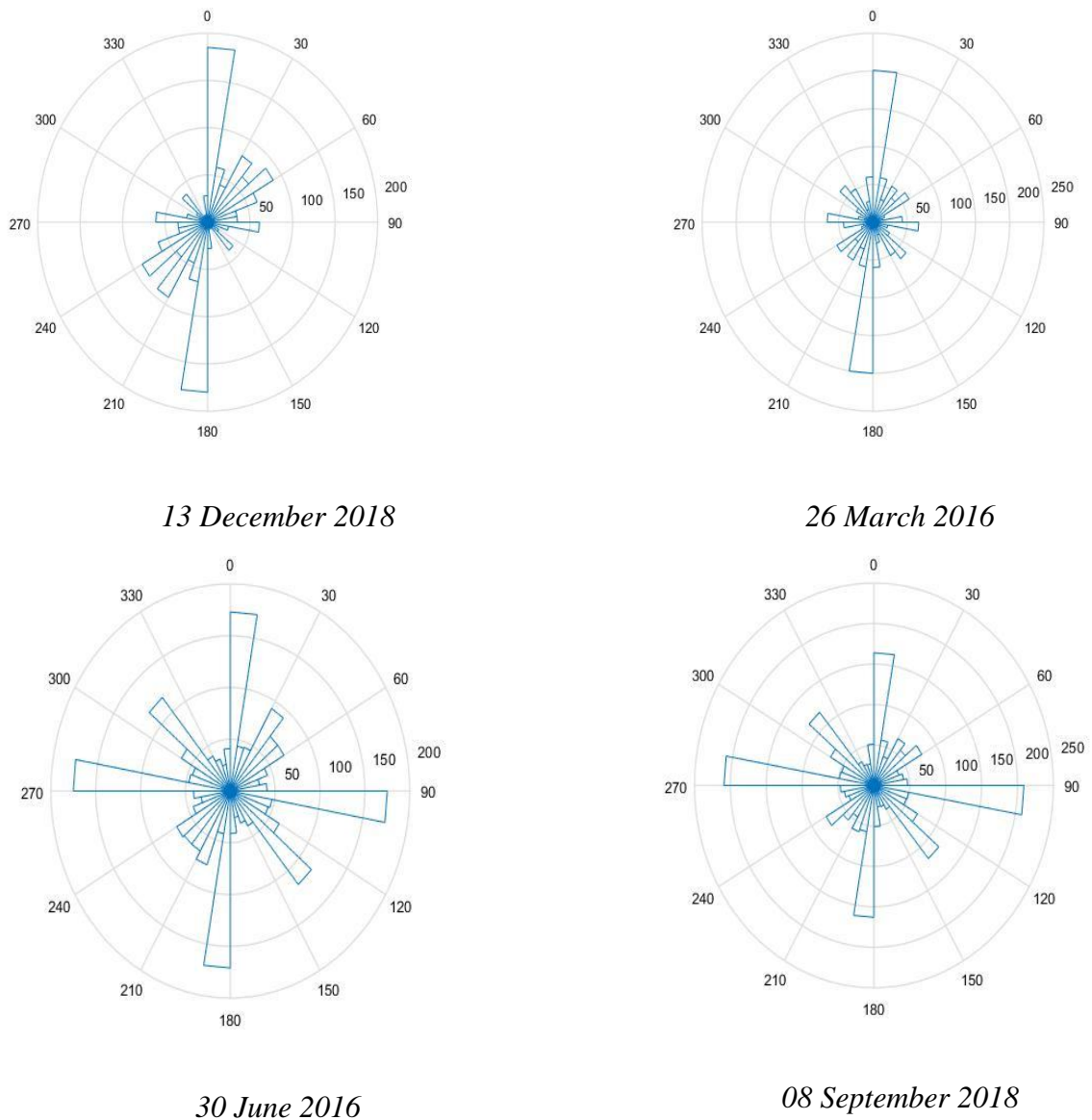
Fig. 2. Histograms of statistics length of lineaments

Table 2. Histograms of statistics length of lineaments

Value	December	March	June	September
Count	2250	4946	4821	4977
Minimum, m	30	42,426407	30	60
Maximum, m	4031,178488	3660,737631	3606,244584	4494,997219
Sum, m	1952567,789889	3919342,472587	3694166,213857	3665247,540268
Standard Deviation, m	476,465568	426,627439	428,331906	406,558094

Analysis of the lineament network for different time periods images allows highlighting of the orientation of them (fig. 3). The interpretation of all lineaments allowed dominance of N–S as a main lineament direction and W–E striking as a secondary lineament direction for whole territory. N–S orientation of the lineaments is all periods and may indicate the trend of the fault movement in the region [Burtman, 2019]. W–E orientation dominates during high water capacity periods (June, September) and may indicate water level variation effect.

Lineament density maps for the study area present the concentrations of the lineaments near the Charvak reservoir more detailed (fig. 4). It appears from all maps that there are several zones in the area. The resulting lineament density maps show dominantly increased density towards the southeastern part of the area. In the northern part of the area, there is a high concentration of lineaments for winter-spring period; that seems to be the result of high effectively of the seasonal (snow pack, rainfall) processes. The lineaments density maps for June and September can clear reflect faults arising from water level fluctuations.



*Fig. 3. Rose diagrams showing the main trends for the observed lineaments*

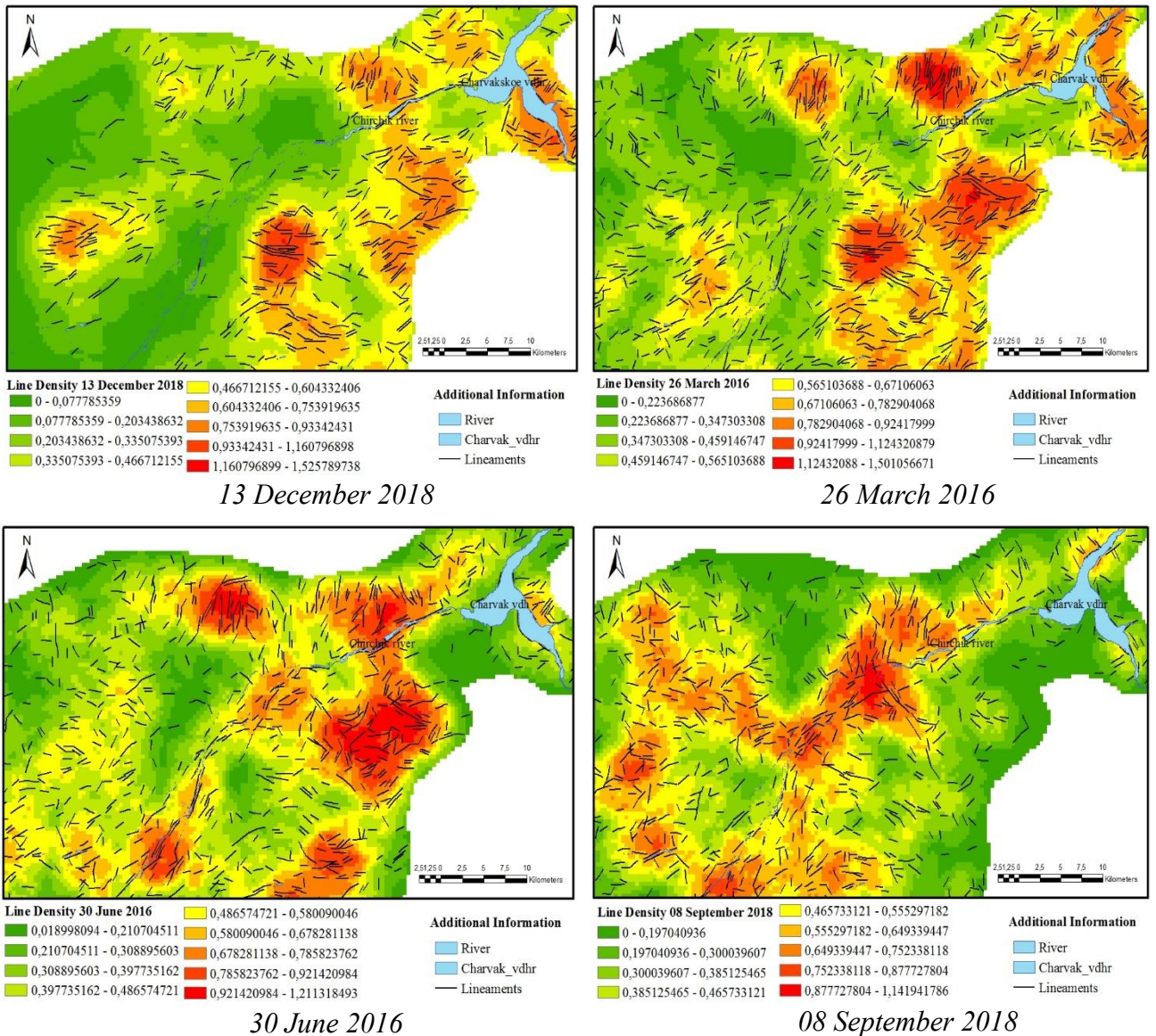


Fig. 4. Lineament density map

## CONCLUSIONS

This study was conducted to characterize and to analyze the spatial organization of lineaments in the vicinity of the Charvak reservoir. The Landsat-8 images with 30 m resolution of the study region from the USGS Earth Explorer website were obtained for special (top water level, downstream, fully drawn down) time periods in the Charvak reservoir (December, March, June and September). Automated lineament analysis methodology was used in this research. ENVI, PCI Geomatica and ArcGIS software were used for data processing. Results show that the minimum of lineaments number reached in December month (2250) during reservoir end of water downstream time. In contrast, March, June and September are periods with high numbers of lineaments. We concluded that water level fluctuations have a greater influence on the appearance of the lineaments structure than periods of water filling and downstream in the reservoir. The lineaments density maps for summer-autumn periods showed the faults arising from water level fluctuations only. Winter-spring period affected with high influence of the seasonal (snow pack, rainfall) processes as well.

## ACKNOWLEDGEMENTS

This work was carried out within the scientific and applied project FA-A5-F014 of the Astronomical Institute of Uzbekistan with the financial support of the Ministry of Innovative Development of the Republic of Uzbekistan.

## REFERENCES

1. *Bondur V.G., Krapivin V.F., Savinykh V.P.* Monitoring and forecasting natural disasters. Moscow: Scientific World, 2009. 692 p. (in Russian).
  2. *Burtman V.* Disjunctive dislocations of the upper crust of Tien Shan. Reports Earth Sciences, 2019. V. 484. P. 37–39. DOI: 10.1134/S1028334X19010185.
  3. *Chaabouni R., Bouaziz S., Peresson H., Wolfgang J.* Lineament analysis of South Jene in Area (Southern Tunisia) using remote sensing data and geographic information system. The Egyptian Journal of Remote Sensing and Space Sciences, 2012. V. 15. P. 197–206.
  4. *Gubin V.N.* Satellites technology in geodynamics. Minsk: Minsktipproekt, 2010. 87 p. (in Russian).
  5. *Lillesand T.M., Kiefer R.W., Chipman J.W.* Remote Sensing and Image Interpretation. 5<sup>th</sup> edition. New York: John Wiley & Sons Inc., 2004. 666 p. DOI: 10.2307/634969.
  6. Geomatica 2013. OrthoEngine. Course Exercises. Version 2013. Richmond Hills, Ontario, Canada: PCI Geomatics Enterprises Inc., 2013. 169 p.
  7. *Prabhakaran A.N., Jawahar Ray N.* Mapping and analysis of tectonic lineaments of Pachamalai hills, Tamil Nadu, India using geospatial technology. Geology, Ecology, and Landscapes, 2018. 22 Mar. P. 81–103. DOI: 10.1080/24749508.2018.1452481.
  8. *Rakhmatullaev Sh., Huneau F., Celle-Jeanton H., Le Coustumer Ph., Motelica-Heino M., Bakiev M.* Water reservoirs, irrigation and sedimentation in Central Asia: A first cut assessment for Uzbekistan. Environmental Earth Sciences, 2013. No 68 (4). P. 985–998. DOI: 10.1007/s12665-012-1802-0.
  9. *Roy D.P., Wulder M.A., Loveland T.R., Woodcock C.E., Allen R.G., Anderson M.C.* Landsat-8: science and product vision for terrestrial global change research Remote Sens. Environ, 2014. No 145. P. 154–172.
  10. *Takorabt M., Toubal A.C., Haddoum H., Zerrouk S.* Determining the role of lineaments in underground hydrodynamics using Landsat 7 ETM+ data, case of the Chott El Gharbi Basin (western Algeria). Arabian Journal of Geosciences, 2018. No 11 (76). DOI: 10.1007/s12517-018-3412-y.
  11. *Yarmukhamedov A.R., Yakubov D.H., Sattarov A.S.* Modern geodynamics of East Uzbekistan. Tashkent: “Fan”, 1979. 111 p. (in Russian).
-